

Synthesis of the superlattice complex oxide Sr₅Bi₄Ti₈O₂₇ and its band gap behavior

M. A. Zurbuchen, N. J. Podraza, J. Schubert, Y. Jia, and D. G. Schlom

Citation: [Applied Physics Letters](#) **100**, 223109 (2012); doi: 10.1063/1.4722942

View online: <http://dx.doi.org/10.1063/1.4722942>

View Table of Contents: <http://scitation.aip.org/content/aip/journal/apl/100/22?ver=pdfcov>

Published by the [AIP Publishing](#)

Articles you may be interested in

[Compositional engineering of BaTiO₃/\(Ba,Sr\)TiO₃ ferroelectric superlattices](#)

J. Appl. Phys. **114**, 104102 (2013); 10.1063/1.4820576

[Strain effect in PbTiO₃/PbZr_{0.2}Ti_{0.8}O₃ superlattices: From polydomain to monodomain structures](#)

J. Appl. Phys. **112**, 114102 (2012); 10.1063/1.4767329

[Structural and ferroelectric properties of epitaxial Bi₅Ti₃FeO₁₅ and natural-superlattice-structured Bi₄Ti₃O₁₂ – Bi₅Ti₃FeO₁₅ thin films](#)

J. Appl. Phys. **108**, 074106 (2010); 10.1063/1.3491023

[Natural-superlattice-structured Bi₄Ti₃O₁₂ – SrBi₄Ti₄O₁₅ ferroelectric thin films](#)

Appl. Phys. Lett. **82**, 784 (2003); 10.1063/1.1543248

[Structural and dielectric properties of epitaxial Ba_{1-x}Sr_xTiO₃ / Bi₄Ti₃O₁₂ / ZrO₂ heterostructures grown on silicon](#)

Appl. Phys. Lett. **77**, 1523 (2000); 10.1063/1.1290724

Want to publish your paper in the
#1 MOST CITED journal in applied physics?

With *Applied Physics Letters*, you can.

AIP | Applied Physics
Letters

THERE'S POWER IN NUMBERS. Reach the world with AIP Publishing.



Synthesis of the superlattice complex oxide $\text{Sr}_5\text{Bi}_4\text{Ti}_8\text{O}_{27}$ and its band gap behavior

M. A. Zurbuchen,^{1,a)} N. J. Podraza,² J. Schubert,³ Y. Jia,⁴ and D. G. Schlom⁴

¹*Department of Materials Science and Engineering, University of California, Los Angeles 90095, USA*

²*Department of Physics and Astronomy, University of Toledo, Toledo, Ohio 43606, USA*

³*Peter Grünberg Institute, JARA-Fundamentals of Future Information Technologies, Research Centre Jülich, D-52425 Jülich, Germany*

⁴*Department of Materials Science and Engineering and Kavli Institute at Cornell for Nanoscale Science, Cornell University, Ithaca, New York 14853, USA*

(Received 13 April 2012; accepted 14 May 2012; published online 31 May 2012)

The $n = 8$ member of the Aurivillius complex oxide superlattice series of phases, $\text{Sr}_5\text{Bi}_4\text{Ti}_8\text{O}_{27}$, was synthesized by pulsed-laser deposition on (001) SrTiO_3 single-crystal substrates. This phase, with a c -axis lattice parameter of 7.25 ± 0.036 nm, and its purity were confirmed by x-ray diffraction and transmission electron microscopy. The film is observed to be single phase and free of intergrowths of other- n members of the series. Using spectroscopic ellipsometry, $\text{Sr}_5\text{Bi}_4\text{Ti}_8\text{O}_{27}$ was determined to exhibit an indirect band gap of 3.53 eV at room temperature. © 2012 American Institute of Physics. [<http://dx.doi.org/10.1063/1.4722942>]

Aurivillius phases¹ represent an important class of complex oxides exhibiting numerous properties of interest for microelectronic applications, as well as physically significant behaviors. They are an ideal platform for study of reduced-dimensionality effects due to their superlattice layering.² Aurivillius phases exhibit ferroelectric transitions,^{3,4} and some doped forms exhibit ferromagnetic transitions.⁵ They are used in nonvolatile memories, and have been considered for use as high- k dielectric layers.⁶ Their thermal behavior exhibits significant anisotropy,⁷ and has led to their consideration as solid-state insulators for microelectronic applications. Bismuth-based oxides have attractive photocatalytic properties under visible light.⁸

These nanostructured materials are represented by the formula $(\text{Bi}_2\text{O}_2)(\text{A}_{n-1}\text{B}_n\text{O}_{3n+1})$, and consist crystallographically of $\text{Bi}_2\text{O}_2^{2+}$ -type pyramidal layers interleaved with n number of ABO_3 -type perovskite blocks. Exploration of previously unsynthesized members of this series is a promising approach to realizing improved properties and extending our understanding of the behavior of such oxide superlattices. Previous studies of oxide superlattice phases have found crossovers in behaviors such as thermal transport⁹ and ferromagnetism to paramagnetism.¹⁰

Thermodynamics limits single-crystal and bulk growth of many Aurivillius phases, particularly with increasing n (increasing superlattice period).¹¹ Large-period layered oxides of a given series will have nearly identical formation energies, due to the minimal compositional variation from one high- n member and the next. In a free-energy versus composition diagram, slopes of the phase coexistence tangents differ very little from n to $n+1$, essentially merging into an envelope at high n and providing a weak driving force for structural rearrangement,¹² therefore requiring stable temperature control at the very least. Calculations on the structurally related Ruddlesden-Popper phases have shown that in the bulk, an

intergrowth of multiple- n members is the most stable microstructure,¹³ and such considerations could apply similarly to high- n Aurivillius phases such as the one under study. The constraint imposed by epitaxial growth is used to stabilize this high- n member, inaccessible by other routes. The authors are not aware of previous synthesis of $\text{Sr}_5\text{Bi}_4\text{Ti}_8\text{O}_{27}$ in any form—polycrystalline or single crystalline.

There is considerable disagreement regarding the band gaps of the related $n = 3$ Aurivillius phase $\text{Bi}_4\text{Ti}_3\text{O}_{12}$ from previous ellipsometric studies. A broad range of band gap energies has been reported, from 3.0 to 3.64 eV,^{14–20} highly dependent upon processing conditions, sample thickness, and possible porosity, even when surface roughness is taken into account.¹⁸ Similar disagreement exists in reports of the La-doped $n = 3$ Aurivillius phase $\text{Bi}_{3.25}\text{La}_{0.75}\text{Ti}_3\text{O}_{12}$.^{21,22} The bandgap of polycrystalline $\text{Bi}_4\text{Ti}_3\text{O}_{12}$ has also been studied;¹⁶ microstructure is known to have significant impact on band gap behavior.²³ Further, most studies were on films that were also only partially oriented, forcing an assumption of isotropic behavior. The most reliable values in the literature for $\text{Bi}_4\text{Ti}_3\text{O}_{12}$ are considered to be 3.18 eV, as measured on an epitaxial film of $\text{Bi}_4\text{Ti}_3\text{O}_{12}$ (001) deposited on SrTiO_3 (001) by chemical vapor deposition,¹⁹ though the authors note that this value is likely blue-shifted due to the film being under tensile strain,²⁴ and 2.9 eV indirect (3.1 eV direct) for $\text{Bi}_4\text{Ti}_3\text{O}_{12}$ (001) deposited on SrTiO_3 (001) by pulsed-laser deposition (PLD).¹⁷

In this manuscript, we describe the synthesis by PLD of an epitaxial $n = 8$ member of the Aurivillius series, $\text{Sr}_5\text{Bi}_4\text{Ti}_8\text{O}_{27}$, enabled by a pseudo-blackbody cavity furnace and precise control of temperature. Phase purity was confirmed and the microstructure characterized by x-ray diffraction (XRD) and transmission electron microscopy (TEM), as well as confirming that the film was fully dense and epitaxial. The complex dielectric function ($\epsilon = \epsilon_1 + i\epsilon_2$) spectra, the resulting optical band gap behavior of the material, film thickness, and surface roughness layer thickness were measured by

^{a)}Electronic mail: mark_z@mac.com.

spectroscopic ellipsometry. The epitaxial nature of the film and the high confidence interval for the ellipsometric microstructural model yield results that are considered accurate for this fundamental material property measurement of $\text{Sr}_5\text{Bi}_4\text{Ti}_8\text{O}_{27}$.

Thin films were grown in a radiatively heated PLD chamber,²⁵ which limits thermal variations across the surface of the substrate. PLD targets were prepared by milling high-purity powders of Bi_2O_3 , TiO_2 , and SrCO_3 of at least 99.99% purity and sintering in air, adding 15% excess bismuth oxide to provide an overpressure of bismuth during PLD growth from the single target. Film growths were performed by 10 000 pulses of a KrF excimer laser ($\lambda = 248$ nm) at 10 pulses/s and a fluence of 2–6 J/cm^2 onto SrTiO_3 (001) substrates at temperatures from $750\text{--}780^\circ\text{C} \pm 0.1^\circ\text{C}$ (precision of readout as measured by a type N thermocouple) under 90 mTorr of molecular oxygen using a pseudo-blackbody substrate heater.²⁵ Films were quenched immediately after growth to avoid bismuth sub-oxide volatilization, which has been shown to lead to microstructural degradation in the absence of quenching.²⁶ Phase purity was studied by XRD, and was confirmed by TEM on a focused ion beam (FIB)-prepared lamella (FEI Nova 600) using an FEI Titan microscope operated at 300 keV. Films were studied by *ex situ* spectroscopic ellipsometry at room temperature at four angles of incidence, $\Theta_i = 50^\circ, 60^\circ, 70^\circ$, and 80° , using a variable-angle multichannel spectroscopic ellipsometer based on dual rotating compensators²⁷ over a spectral range from 0.75 to 5.15 eV.

A θ - 2θ XRD scan of the (0021)-oriented $\text{Sr}_5\text{Bi}_4\text{Ti}_8\text{O}_{27}$ film is shown in Fig. 1. Most superlattice peaks for 00ℓ , with ℓ even, from 002 through 0058 are clearly resolved, indicating a high degree of long-range order in the film. The c -axis lattice parameter was determined by a Nelson-Riley analysis²⁸ to be 7.25 ± 0.036 nm, in agreement with estimates based on addition of structural subunits. There is no appearance of odd ℓ peaks or of splitting of the peaks, which would have been an indication of other- n intergrowths²⁹ or a high density of out-of-phase boundary (OPB) planar defects.³⁰ The out-of-plane orientation relationship is SrTiO_3 (001)|| $\text{Sr}_5\text{Bi}_4\text{Ti}_8\text{O}_{27}$ (001).

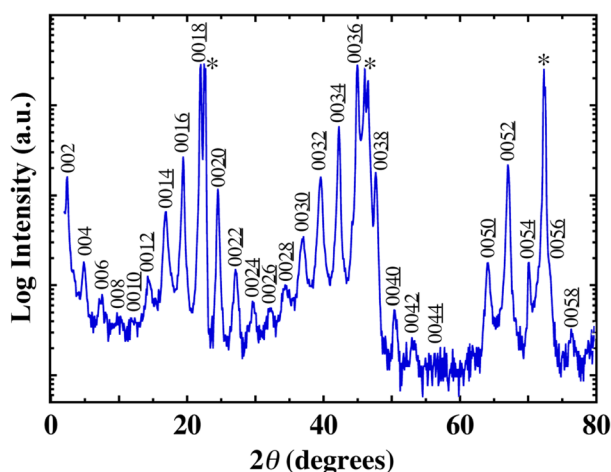


FIG. 1. θ - 2θ XRD scan of the $\text{Sr}_5\text{Bi}_4\text{Ti}_8\text{O}_{27}$ (001)/ SrTiO_3 (001) film, exhibiting only 00ℓ ($\ell = \text{even}$) peaks associated with the superlattice and the substrate phase. * indicate substrate peaks.

As described elsewhere, analysis by TEM is required to verify the synthesis of a high- n (long-period) superlattice phase such as this.³¹ Figure 2(a) shows a $[100]_{\text{substrate}}$ cross-sectional phase-contrast TEM image, and Fig. 2(b) shows a $[100]_{\text{substrate}}$ -type electron diffraction pattern taken using parallel illumination of an approximately 100 nm spot in a thick region of the same sample. Periodic layering is clear. The in-plane orientation relationship is SrTiO_3 $[100] \parallel \text{Sr}_5\text{Bi}_4\text{Ti}_8\text{O}_{27}$ $[100]$, assuming the unit cell of $\text{Sr}_5\text{Bi}_4\text{Ti}_8\text{O}_{27}$ is its paraelectric tetragonal prototype cell.³² Extra spots are, however, present in the diffraction pattern, and are considered to be due to double-diffraction, or possibly that the phase may have undergone transformation to a lower-symmetry form. Even- n Aurivillius phases are known to undergo a "puckering" of pairs of titania octahedra in the perovskite slab (oppositional tilting about an axis perpendicular to the layering axis), maintaining mirror symmetry along c , but breaking rotational symmetry along b , to typically reduce the unit cell-type from $I4/mmm$ to orthorhombic $A2_1am$.³³ The

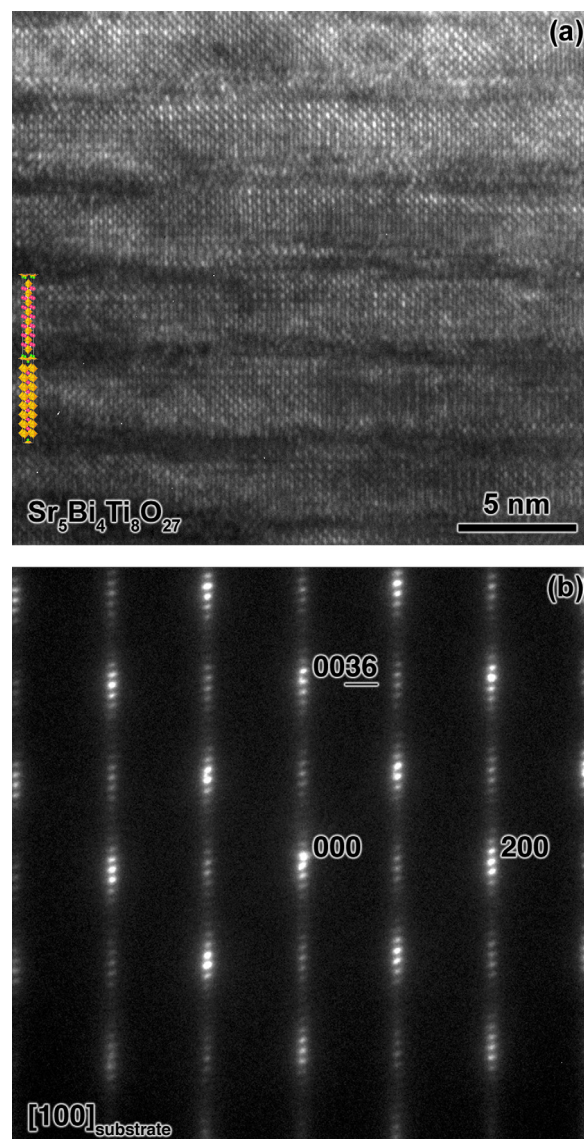


FIG. 2. (a) Cross-sectional phase-contrast TEM image of the same $\text{Sr}_5\text{Bi}_4\text{Ti}_8\text{O}_{27}$ film studied in Fig. 1, showing periodic $n = 8$ layering, with a scaled schematic of the structure inset. (b) A zone-axis nano-diffraction pattern of the same cross-section of the $\text{Sr}_5\text{Bi}_4\text{Ti}_8\text{O}_{27}$ film, showing well-defined superlattice reflections.

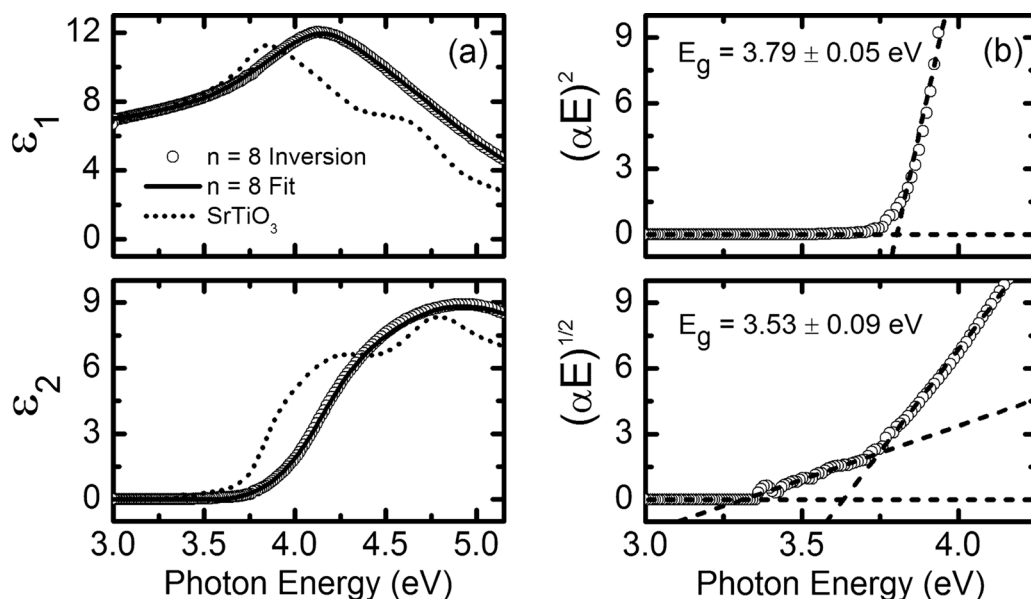


FIG. 3. (a) Comparison of the complex dielectric function spectra ($\epsilon = \epsilon_1 + i\epsilon_2$) of $\text{Sr}_5\text{Bi}_4\text{Ti}_8\text{O}_{27}$ obtained by numerical inversion (open circles) and parameterization (solid line). ϵ for SrTiO_3 data is shown for comparison (dotted line). (b) Plots of $(\alpha E)^2$ and $(\alpha E)^{1/2}$ as functions of photon energy for $\text{Sr}_5\text{Bi}_4\text{Ti}_8\text{O}_{27}$. Dashed lines are linear fits to regions of the data.

specific details remain the subject for a future variable-temperature diffraction investigation.

The dielectric function ϵ and microstructural parameters were extracted (for the same film studied by XRD analysis) using a least-squares regression analysis and an unweighted error function,³⁴ to fit the experimental ellipsometric spectra (in Δ , ψ) collected at all four angles of incidence to an optical model consisting of a semi-infinite SrTiO_3 substrate/bulk $\text{Sr}_5\text{Bi}_4\text{Ti}_8\text{O}_{27}$ film/surface roughness/air ambient structure, where free parameters correspond to the bulk and surface roughness thicknesses of the film, and a parameterization of ϵ for $\text{Sr}_5\text{Bi}_4\text{Ti}_8\text{O}_{27}$ over a spectral range from 2.5 to 5.15 eV. A thickness gradient was incorporated into the model to quantify thin film thickness uniformity over the size of the ellipsometer beam spot (~ 3 mm in diameter), resulting in the need for the reduced spectral range in modeling. ϵ was parameterized by two Tauc-Lorentz oscillators³⁵ sharing a common absorption onset, and a high-energy Sellmeier oscillator.³⁶ The optical properties of the surface roughness layer were represented by a Bruggeman effective medium approximation³⁷ consisting of a 50% bulk film/50% void mixture, based on our previous observations of formula-unit crystallization of related high- n Aurivillius phases. The average film thickness was determined to be 171 ± 0.2 nm, and the roughness 3.22 ± 0.1 nm, in agreement with the observed formula-unit surface-step morphology.

Numerical inversion was used to extract ϵ directly from the $\Theta_i = 70^\circ$ Δ , ψ spectra using the bulk layer and surface roughness thicknesses deduced from the parameterized fit. Figure 3(a) shows ϵ for $\text{Sr}_5\text{Bi}_4\text{Ti}_8\text{O}_{27}$, obtained from inversion and parameterization, and compared to previously determined SrTiO_3 spectra. Overall, ϵ for $\text{Sr}_5\text{Bi}_4\text{Ti}_8\text{O}_{27}$ exhibits fewer and broader critical point features. Above the band gap of SrTiO_3 , $\text{Sr}_5\text{Bi}_4\text{Ti}_8\text{O}_{27}$ exhibits lower absorption, indicating a higher band gap.

The absorption coefficient, α , was obtained from the numerically inverted ϵ . $(\alpha E)^{1/2}$ and $(\alpha E)^2$ were plotted as

functions of photon energy (E), and extrapolated using a linear relationship to $(\alpha E)^{1/2}$ [$(\alpha E)^2$] = 0 to identify the indirect and direct band gaps,³⁸ as shown in Fig. 3(b). The criteria for an indirect band gap includes the presence of two slopes for $\alpha^{1/2} = 0$ in order to account for the contribution from phonons,³⁸ and the average of the intercepts of these two slopes indicates the band gap. In this situation, the results of Fig. 3(b) indicate that $\text{Sr}_5\text{Bi}_4\text{Ti}_8\text{O}_{27}$ possesses a direct gap of 3.79 ± 0.05 eV and an indirect gap of 3.53 ± 0.09 eV. Compared to literature values for the related $n = 3$ $(\text{Bi},\text{La})_4\text{Ti}_3\text{O}_{12}$ and $\text{Bi}_4\text{Ti}_3\text{O}_{12}$ Aurivillius phases, we observe a larger band gap. The direct gap for SrTiO_3 at ~ 3.8 – 3.9 eV is relatively close to the direct gap of $\text{Sr}_5\text{Bi}_4\text{Ti}_8\text{O}_{27}$, while the indirect gap for SrTiO_3 at ~ 3.1 – 3.2 eV is substantially lower. The physics responsible for these observations are not yet clear, and the authors suggest that similar experiments on a series of n -values of related Aurivillius phases could provide further insight.

In summary, epitaxial thin films of the $n = 8$ Aurivillius phase $\text{Sr}_5\text{Bi}_4\text{Ti}_8\text{O}_{27}$ have been synthesized by PLD. Structure and epitaxy were confirmed by XRD and cross-sectional TEM imaging and diffraction. Spectroscopic ellipsometry indicates that $\text{Sr}_5\text{Bi}_4\text{Ti}_8\text{O}_{27}$, with an indirect gap at 3.53 eV, has optical behavior significantly different from SrTiO_3 .

This work was supported by the Defense Advanced Research Projects Agency (DARPA) and the U.S. Army Aviation and Missile Research, Development, and Engineering Center (AMRDEC).³⁹ Sample preparation was performed by the UCLA Nanoelectronics Research Facility, and microscopy at the UCLA California Nanosystems Institute's (CNSI's) Electron Imaging Center for Nanomachines (EICN).

¹B. Aurivillius, *Ark. Kemi* **1**, 463 (1950); **1**, 499 (1950); **2**, 519 (1951); **5**, 39 (1953); B. Aurivillius and P. H. Fang, *Phys. Rev.* **126**, 893 (1962).

²D. G. Schlom, L.-Q. Chen, X. Q. Pan, A. Schmehl, and M. A. Zurbuchen, *J. Am. Ceram. Soc.* **91**, 2429 (2008).

³E. C. Subbarao, *Phys. Rev.* **122**, 804 (1961).

- ⁴E. C. Subbarao, *J. Phys. Chem. Solids* **23**, 665 (1962).
- ⁵M. A. Zurbuchen, R. S. Freitas, M. J. Wilson, P. Schiffer, M. Roeckerath, J. Schubert, G. H. Mehta, D. J. Comstock, J. H. Lee, Y. Jia, and D. G. Schlom, *Appl. Phys. Lett.* **91**, 033113 (2007).
- ⁶Y. Sakashita and H. Funakubo, U.S. patent 7,145,158 (2006); Y. Sakashita and H. Funakubo, U.S. patent 7,242,044 (2007).
- ⁷Y. Shen, D. R. Clarke, and P. A. Fuierer, *Appl. Phys. Lett.* **93**, 102907 (2008).
- ⁸T. Saison, N. Chemin, C. Chanéac, O. Durupthy, V. Ruaux, L. Mariey, F. Maugé, P. Beaunier, and J.-P. Jolivet, *J. Phys. Chem. C* **115**, 5657 (2011).
- ⁹A. Chernatynskiy, R. W. Grimes, M. A. Zurbuchen, D. R. Clarke, and S. R. Phillpot, *Appl. Phys. Lett.* **95**, 161906 (2009).
- ¹⁰T. M. Rice and M. Sigrist, *J. Phys.: Condens. Matter* **7**, L643 (1995).
- ¹¹M. A. Zurbuchen, J. Lettieri, G. Asayama, Y. Jia, S. Knapp, A. H. Carim, D. G. Schlom, X. Q. Pan, and S. K. Streiffer, *J. Mater. Res.* **22**, 1439 (2007).
- ¹²J. S. Anderson, in *The Chemistry of Extended Defects in Non-metallic Solids: Proceedings of the Institute for Advanced Study on the Chemistry of Extended Defects in Non-metallic Solids*, edited by L. Eyring and M. O'Keefe (North-Holland, Amsterdam, The Netherlands, 1970), pp. 1–20.
- ¹³W. Tian, X. Q. Pan, J. H. Haeni, and D. G. Schlom, *J. Mater. Res.* **16**, 2013 (2001).
- ¹⁴S. Ehara, K. Muramatsu, M. Shimazu, J. Tanaka, M. Tsukioka, Y. Mori, T. Hattori, and H. Tamura, *Jpn. J. Appl. Phys.* **20**, 877 (1981).
- ¹⁵H. S. Gu, D. H. Bao, S. M. Wang, D. F. Gao, A. X. Kuang, and X. J. Li, *Thin Solid Films* **283**, 81 (1996).
- ¹⁶C. Jia, Y. Chen, and W. F. Zhang, *J. Appl. Phys.* **105**, 113108 (2009).
- ¹⁷D. J. Singh, S. S. A. Seo, and H.-N. Lee, *Phys. Rev. B* **82**, 180103 (2010).
- ¹⁸J. Zhang, X. Chen, K. Jiang, Y. Shen, Y. Li, Z. Hu, and J. Chu, *Dalton Trans.* **40**, 7967 (2011).
- ¹⁹S. Bin-Anooz, J. Schwartzkopf, P. Petrik, M. Schmidbauer, A. Duk, E. Agocs, and R. Fornari, *Appl. Phys. A* **105**, 81 (2011).
- ²⁰W. S. Choi, M. F. Chisolm, D. J. Singh, T. Choi, G. E. Jellison, Jr., and H.-N. Lee, *Nat. Commun.* **3**, 689 (2012).
- ²¹Z. Hu, G. Wang, Z. Huang, and J. Chu, *J. Appl. Phys.* **93**, 3811 (2003).
- ²²G. S. Wang, X. J. Meng, Z. Q. Lai, J. Yu, J. L. Sun, S. L. Guo, and J. H. Chu, *Appl. Phys. A: Mater. Sci. Process.* **76**, 83 (2003).
- ²³S. Trolier-McKinstry, J. Y. Chen, K. Vedam, and R. E. Newnham, *J. Am. Ceram. Soc.* **78**, 1907 (1995).
- ²⁴C. Himcinschi, I. Vrejoiu, M. Friedrich, E. Nikulina, L. Ding, C. Cobet, N. Esser, M. Alexe, D. Rafaja, and D. R. T. Zahn, *J. Appl. Phys.* **107**, 123524 (2010).
- ²⁵J. C. Clark, J.-P. Maria, K. J. Hubbard, and D. G. Schlom, *Rev. Sci. Instrum.* **68**, 2538 (1997).
- ²⁶M. A. Zurbuchen, J. Lettieri, S. J. Fulk, Y. Jia, A. H. Carim, D. G. Schlom, and S. K. Streiffer, *Appl. Phys. Lett.* **82**, 4711 (2003).
- ²⁷C. Chen, I. An, G. M. Ferreira, N. J. Podraza, J. A. Zapien, and R. W. Collins, *Thin Solid Films* **455–456**, 14 (2004).
- ²⁸J. B. Nelson and D. P. Riley, *Proc. Phys. Soc. London* **57**, 160 (1945).
- ²⁹V. S. Kopp, V. M. Kaganer, J. Schwarzkopf, F. Waidick, T. Remmele, A. Kwasniewski, and M. Schmidbauer, *Acta Crystallogr. A* **68**, 148 (2012).
- ³⁰M. A. Zurbuchen, W. Tian, X. Q. Pan, D. Fong, S. K. Streiffer, M. E. Hawley, J. Lettieri, Y. Jia, G. Asayama, S. J. Fulk, D. J. Comstock, S. Knapp, A. H. Carim, and D. G. Schlom, *J. Mater. Res.* **22**, 1439–1471 (2007).
- ³¹M. A. Zurbuchen, V. O. Sherman, A. K. Tagantsev, J. Schubert, M. E. Hawley, D. D. Fong, S. K. Streiffer, Y. Jia, W. Tian, and D. G. Schlom, *J. Appl. Phys.* **107**, 024106 (2010).
- ³²This assumption seems reasonable based on the previously observed downward trend of the paraelectric-to-ferroelectric phase transition temperature (T_C) with increasing n of other members of this $(\text{Bi}_2\text{O}_2)(\text{Sr,Bi})_{n-1}\text{Ti}_n\text{O}_{3n+1} = \text{Bi}_4\text{Ti}_3\text{O}_{12}(\text{SrTiO}_3)_{n-3}$ Aurivillius series of phases.³¹ A T_C of 141 K can be extrapolated from that data for the $n=8$ $\text{Sr}_5\text{Bi}_4\text{Ti}_8\text{O}_{27}$ phase.
- ³³R. E. Newnham, R. W. Wolfe, and J. F. Dorrian, *Mater. Res. Bull.* **6**, 1029 (1971).
- ³⁴Y. Cong, I. An, K. Vedam, and R. W. Collins, *Appl. Opt.* **30**, 2692 (1991).
- ³⁵G. E. Jellison, Jr. and F. A. Modine, *Appl. Phys. Lett.* **69**, 371 (1996); **69**, 2137 (1996).
- ³⁶For example: R. W. Collins and A. S. Ferlauto, in *Handbook of Ellipsometry*, edited by H. G. Tompkins and E. A. Irene, (William Andrew, Norwich, NY, 2005), pp. 125–129.
- ³⁷H. Fujiwara, J. Koh, P. I. Rovira, and R. W. Collins, *Phys. Rev. B* **61**, 10832 (2000).
- ³⁸J. I. Pankov, *Optical Processes in Semiconductors* (Dover, New York, 1975), p. 37.
- ³⁹The views, conclusions contained in this document are those of the authors and should not be interpreted as representing the official policies, either expressed or implied, of the Defense Advanced Research Projects Agency; the U.S. Army Aviation and Missile Research, Development, and Engineering Center; or the U.S. Government.